Int. J. Electrochem. Sci., 11 **(2016)** 2762 - 2777

International Journal of
ELECTROCHEMICAL
SCIENCE
www.electrochemsci.org

In Vitro Bioactivity and Corrosion Properties of Laser Beam Welded Medical Grade AISI 316L Stainless Steel in Simulated Body Fluid

Ceyhun KÖSE[1,*], *Ramazan KAÇAR*[2]

[1]Faculty of Natural Sciences and Engineering, Department of Mechanical Engineering, Gaziosmanpaşa University, Tokat, 60150, Turkey
Tel: +90 356 252 18 00; Fax: +90 356 252 17 29
[2]Faculty of Technology, Department of Manufacturing Engineering, Karabük University, Karabük, 78050, Turkey, Tel +90 370 4338200/1010; Fax: +90 370 433 82 04
[*]E-mail: ceyhunia@gmail.com, ceyhun.kose@gop.edu.tr

Received: 6 January 2016 / *Accepted:* 29 January 2016 / *Published:* 1 March 2016

AISI 316L stainless steel sheet was joined by CO_2 laser beam welding method. In order to determine in vitro bioactivity and corrosion properties of the laser beam welded and non-welded samples were immersed in Simulated Body Fluid (SBF) for 1, 3, 7, 14, 21, 28 days. The bone-like apatite formation was investigated on the surface of the weld area and non-welded samples. Also, corrosion resistance of the laser beam welded and non-welded samples were determined via weight loss method. No corrosion mechanisms were observed in the heat affected zone (HAZ), weld metal of laser beam welded joints, and base material.

Keywords: Biomaterials, Surfaces, Welding, Corrosion test.

1. INTRODUCTION

Modern corrosion resistant (stainless) steel is fabricated by adding more than 12 wt% of chromium (Cr), the addition resulting in the formation of a passive oxide coating on the surface of the alloy [1]. This thin oxide film is characterised by low chemical reactivity and displays a self-healing property in contact with oxygen: this thin oxide layer protects them from corrosion [1]. Nickel (Ni) and molybdenum (Mo) elements are also introduced to stainless steel to improve corrosion, whereas carbon (C) is minimised as C tends to bind to Cr to form chromium carbide, thus minimising the protective anti-corrosion activity of the metal [1,2].

Austenitic stainless steels are the widely used for biomedical industry [1]. The austenitic steels are non-magnetic, and are hardened by means of cold working rather than heat treatment [1]. Their

microstructure provides high corrosion resistance and they have better weldability compared to martensitic and ferritic stainless steel series [1,3]. Stainless steels are biocompatible and has been used as a artificial implant material [4]. 316L austenitic stainless steel is commonly used for biomedical applications [4]. Biocompatibility by being corrosion resistant due to the formation of a protective chromium oxide surface film [4]. 316L stainless steel is widely used in cardiovascular stents, orthodontic wires and orthopedic implants because of its excellent mechanical properties and biocompatibility [5-7].

In the case that stainless steel is used as an orthopedic implant, stainless steels are biologically tolerated and no chemical bonds. Hydroxyapatite (HA) coating deposited on stainless steels improve osseointegration, due to its capacity to form bioactive fixation with the bone tissue [8]. Since metallic implants exhibit bioinert acts or lack having the desired bioactive properties when they are used as implants in the body, they do not interact or bond with any bone tissue, neither positive or negative in the environment they exist [9-11]. The bone-like apatite formation or calcium phosphate (CaP) layer is accepted as a base factor for biomaterials with bioactivity [9].

Hydroxyapatite (HA) is the main inorganic component of bone and teeth and a form of calcium phosphate (CaP) [12-15]. Due to its chemical composition and crystallographic texture, which is similar to living bone, calcium phosphate is in crystallized form. HA ensures bone rigidity and accelerate healing of the bone tissue [9,16-18]. The formation of HA is dependent on temperature, pH and Ca/P ratio, as well as the composition of the SBF solution, detailed preparation procedure of SBF solution [19,20].

In the case that stainless steels are used as an implant material, a disadvantage of stainless steel is its tendency towards corrosion sensitivity under the physiological conditions in the body due to release of metal ions such as those of nickel and chromium [21,22]. Corrosion of stainless steel implants in the human body is critically important because it can negatively affect the biocompatibility [9**,**23]. Corrosion behaviors of biomaterials can be studied using a simulated physiological fluids [24,25].

CO_2 laser beam welding method stands out among the other conventional methods of welding from many aspects such as low heat input, high concentration energy, high welding speed, narrow weld area, deep penetration, automation compliance, high mechanical strength, low distortion and the opportunity to be able to weld without the need of a filler metal [26-31]. Laser beam welding can be used for joining of medical grade stainless steels.

However, there are not any studies about in vitro bioactivity and corrosion properties of laser beam welded stainless steel in simulated body fluid (SBF). Therefore, AISI 316L medical grade stainless steel sheet was performed with CO_2 laser beam welding method in this study. Thus, the SBF was used to evaluate the in vitro bioactivity properties and corrosion resistance of laser beam welded and non-welded samples.

2. EXPERIMENTAL PROCEDURE

2.1. Material and welding application procedure

In this study, AISI 316L stainless steel is widely used in many industries, such as biomedical industry. The chemical composition for the commercially acquired AISI 316L stainless steel is provided (weight %) in Table 1.

Table 1. The chemical composition of AISI 316L stainless steel (weight %).

C %	Si	Mn	P	S	Cr	Mo	Ni	Al	Co
0.013	0.528	1.859	0.052	0.0010	16.94	2.065	9.336	0.0020	0.267
Cu	Nb	Ti	V	W	Pb	Sn	Zn	N	Fe
0.248	0.0338	0.014	0.086	0.099	0.0010	0.026	0.027	0.026	68.36

AISI 316L steel plates were fixed in a horizontal position onto the fixture mold and the welding was performed with the TRUMPF LASERCELL 1005 CO_2 laser beam welding machine of 4 kW capacity without any filler metal and in compliance with the parameters given in Table 2.

Table 2. The welding parameters used for joining AISI 316L stainless steel.

Sample code	Laser power (W)	Travel speed (cm/min)	Shielding gas	Gas flow rate (lt/min)	Focal length (mm)	Heat input (kJ/mm)
A1	3500	90	50% Ar + 50% He	10	200	0.233
A2	3500	180	50% Ar + 50% He	10	200	0.116
A3	3500	270	50% Ar + 50% He	10	200	0.077

2.2. Preparation of the experiment samples and works of characterization

CO_2 laser beam welded AISI 316L stainless steel samples and non-welded samples were prepared in dimensions of 20 x 5 x 3mm and polished with SiC emery papers of meshes between 200 and 1200. This was followed by ultrasonic rinsing in distilled water and acetone for 30 minutes. After the washing process, the samples were dried at 50 ^{o}C in an incubator and the weight of each sample determined before they were put into the SBF solution. The laser beam welded and non-welded samples were immersed for 1, 3, 7, 14, 21, 28 days in the SBF at 37 ^{o}C; the samples were then removed from the SBF, washed with pure water and dried at room temperature, after which their

weight gain (weight gain = (weight after immersion – weight before immersion) / surface area) was measured with a precision scale (0.0001 g.). Then, SEM and EDS were used to characterize the surface morphology of the non-welded samples A and weld seam of laser beam welded samples A1, A2, A3, which were previously immersed in the SBF. After determination of the apatitic calcium formations on the surface, all the samples were cleaned using acidic solution which was prepared in accordance with ASTM G1 and the corrosion products on their surface were removed before weighting [32]. The samples were then weighted to calculate the weight loss (weight loss = (weight before immersion – weight after clean) / surface area). The corrosion rates were calculated according to weight loss as per ASTM G1 [32]. Finally, SEM and EDS were used to characterize the microstructure of non-welded samples A and welded samples A1, A2 and A3, which were immersed in the SBF for 28 days.

2.3. Preparation of the SBF and weight loss corrosion testing experiment

The SBF used in this study was based on the work of Kokubo [33]. While the solution was being prepared the ambient temperature was kept approximately at 37 ^{o}C. SBF chemicals were of the brand Merck and each one of them was added in a certain order and their pH values were adjusted to be 7.4 so that they could be similar to human blood plasma. Chemicals used in the preparation of the SBF solution, their amounts, and order of adding were as such: NaCl, 8.035 g., $NaHCO_3$, 0.355 g., KCL, 0.225 g., K_2HPO_4. $3H_2O$, 0.231 g., $MgCl_2$. $6H_2O$, 0.311 g., 1.0M-HCL, 39 ml., $CaCl_2$, 0.292 g., Na_2SO_4, 0.072 g., Tris, 6.118 g., 1.0M-HCL, 0-5 ml [34]. Both the non-welded and laser beam welded samples were immersed in the SBF solution at 37 °C for 1, 3, 7, 14, 21 and 28 days, respectively. During the experiment period, SBF was changed once in every 2 days and the originality of its ion concentration was preserved. In every soaking period, samples were removed from the SBF, washed with pure water, and dried at room temperature, after which their weight changes were measured with a precision scale. Then, in order to remove the corrosion products on the surface of the laser beam welded and non-welded samples, 100 milliliters of nitric acid (HNO_3) was prepared from the chemical cleaning solutions given in ASTM G1, the samples were then kept for 20 minutes in the bath at 60 ^{o}C, washed with pure water and dried in the oven at 50 ^{o}C in an incubator. The samples were evaluated after they were weighed with the precision scale. Corrosion rate of the laser welded and non-welded samples was calculated by using the weight loss values on the basis of the formula below:

Corrosion Rate (mm/y) = (K x W) / (A x T x D),

where: K = a constant, T = time of exposure in hours, A = area in cm^2, W = mass loss in grams, and D = density in g/cm^3

3. RESULTS AND DISCUSSION

3.1. Weight gain

Fig. 1 shows the weight gain of base material (A) and laser beam welded samples (A1, A2, A3) with 1, 3, 7, 14, 21 and 28 days immersion time.

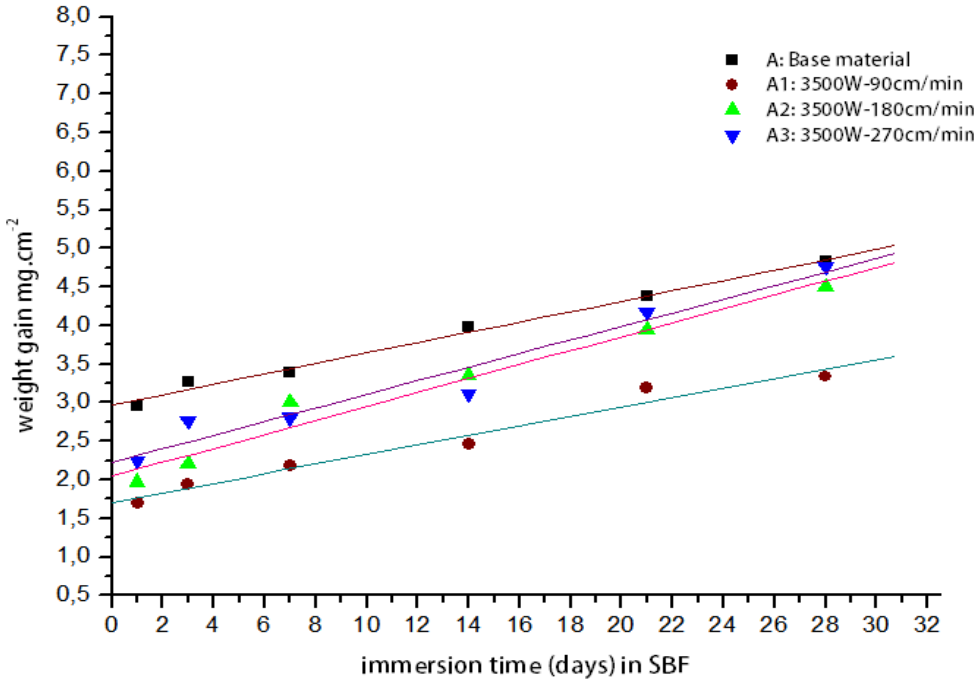

Figure 1. Weight gain rates of the base material (A) and laser beam welded A1, A2 and A3 samples immersed in the SBF for 1-28 days.

Weight gain rises with the increase of the holding time of laser welded and non-welded samples in the SBF (Fig. 1), this is an expected situation. It can be said from the results that the welding thermal cycle directly affects nucleation and growth of apatite on the weld seam surface of the laser welded samples depending on various laser welding speed parameters or various heat inputs. Upon considering the weight gain results of the samples immersed in the SBF for 28 days, it can be clearly concluded from the results that a weight gain occurred due to heat input in the rates of weight gain of the laser beam welded samples. However, when we have a look at the apatite increase rates between the base material and laser beam welded samples, it can be said that the more apatitic calcium was deposited on the surface of the base material. In spite of the base material and samples which were joined by three different laser weld speed parameters immersed in the SBF for the same period, the fact that there are more apatitic calcium deposition on base material shows that a better nucleation and growth of apatite occurred on the surface of the base material than the weld seam surface of welded samples. Either less apatitic formation occurred on the weld seams or apatitic calcium displayed less detachment force (bioadhesive strength) compared to the base material due to being affected by the welding thermal cycle of the laser welded samples which were deposited with apatitic calcium. From these results, we can conclude that bioactivity properties are lower for the weld seam of laser beam welded samples than the surface of the base material.

3.2. Surface morphology

Generally, the apatitic calcium-forming ability of biomaterials can be measured in SBF solutions [20,35].

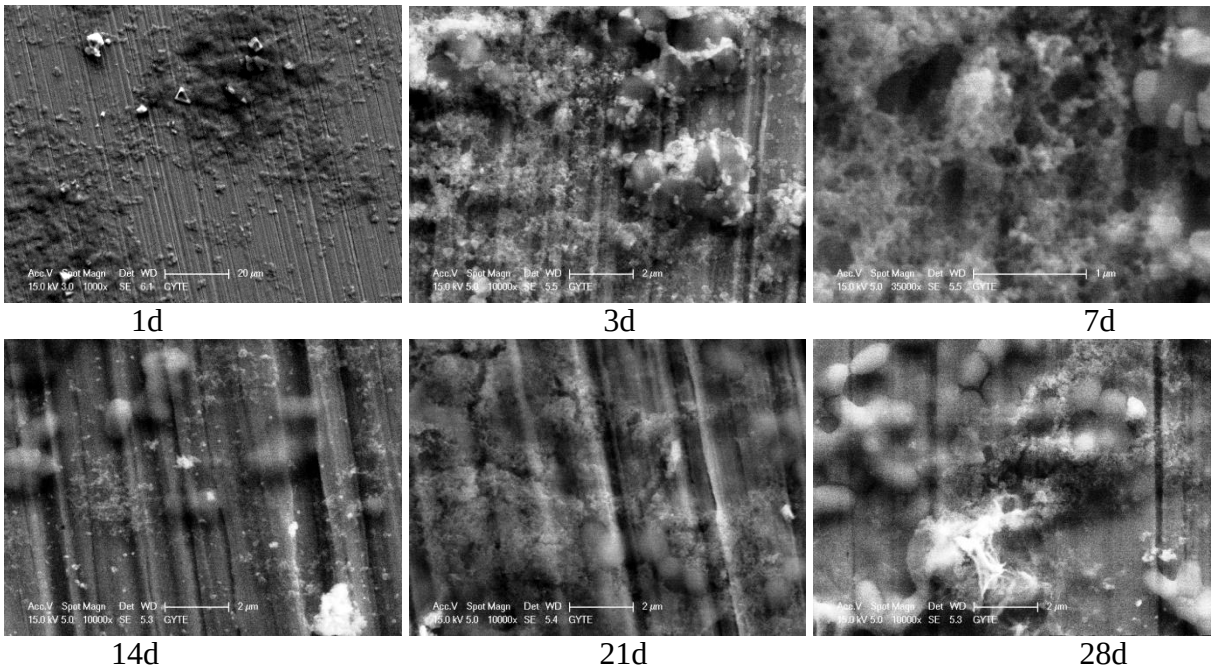

Figure 2. SEM images of the apatite morphology on the weld seam of the laser beam welded A1 sample which was immersed in the SBF for 1 to 28 days.

An implant material's capacity to nucleate and grow apatite on the surface is correlated to the capability of bioactive properties of that material. Materials with apatite formation on their surfaces can also form apatite on the living bone tissue, bone bonding and bone growth can occur on the apatite layer [15]. The apatite-forming ability in the SBF is a measure of in vivo bioactivity [33,36-38]. Bioactivity is described as the capability of the implant material to develop a direct, adherent, and strong bond with the bone tissue [9,15,16,36]. Upon looking at the SEM analysis inspections carried out on the weld seam of the laser welded samples which were coated with apatite, it was determined that the apatite formation generally started on the first day and daily and coated the entire surface of the laser welded and non-welded samples (Fig. 2).

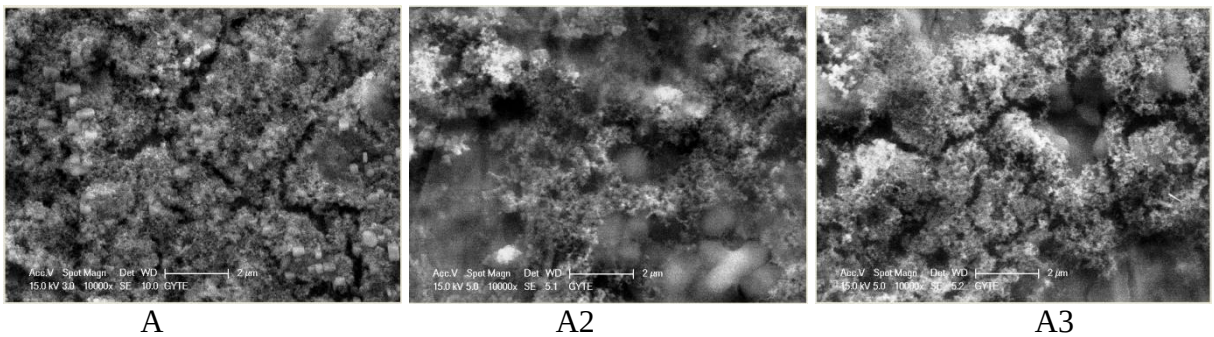

Figure 3. SEM images of the apatite morphology on the A (base material) and weld seam of the laser beam welded A2 and A3 samples on the surface which was immersed in the SBF for 28 days.

Since weld metal and HAZ width in relation to the welding process of the AISI 316L stainless steel samples had different welding parameters and there were different heat inputs, the nucleation and growth of apatite did not show a homogenous distribution on the surfaces. Homogenous distributions on the surfaces were determined by means of the SEM images to have occurred with nano-pore scale apatite morphology. (Fig. 2 and Fig. 3).

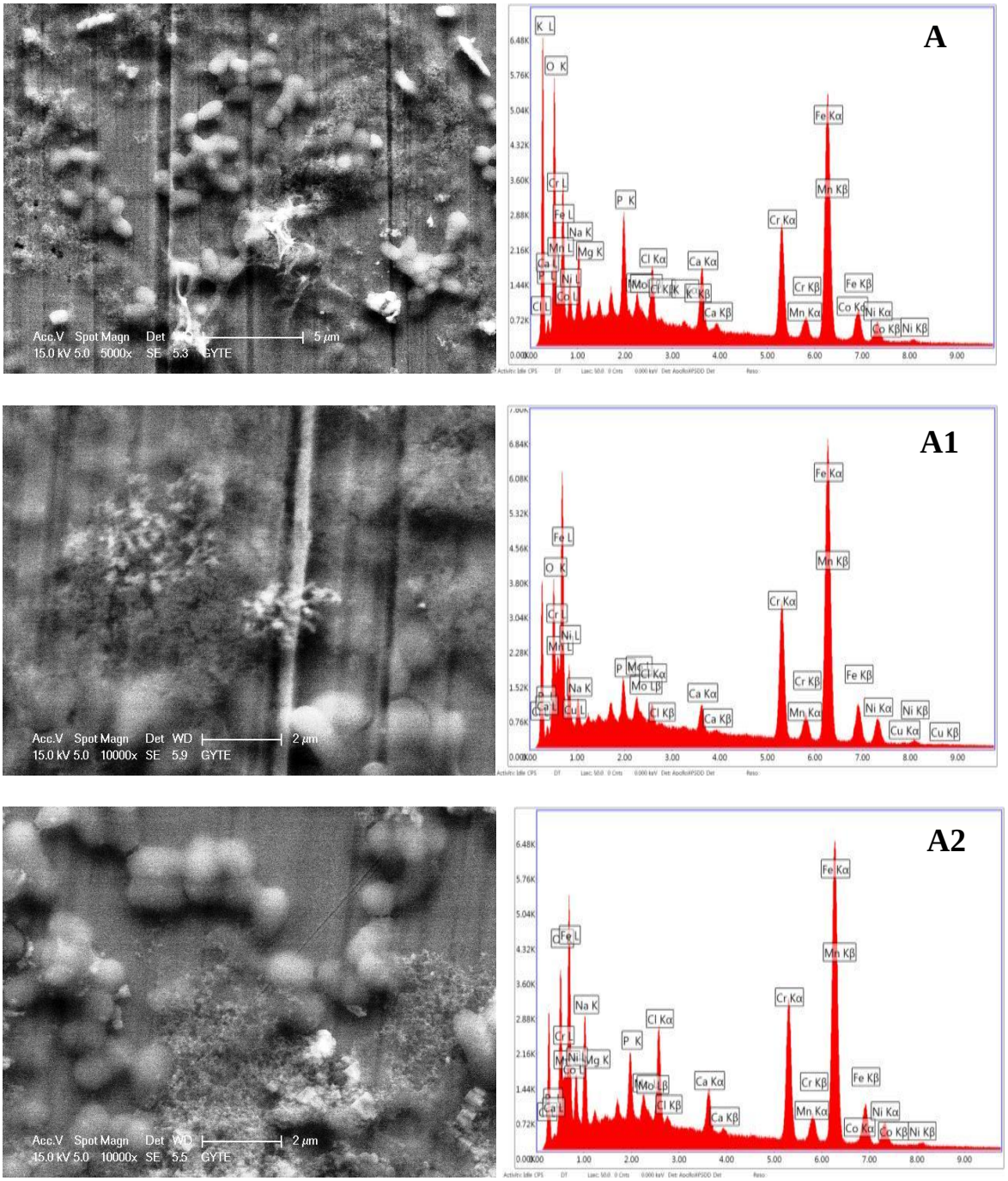

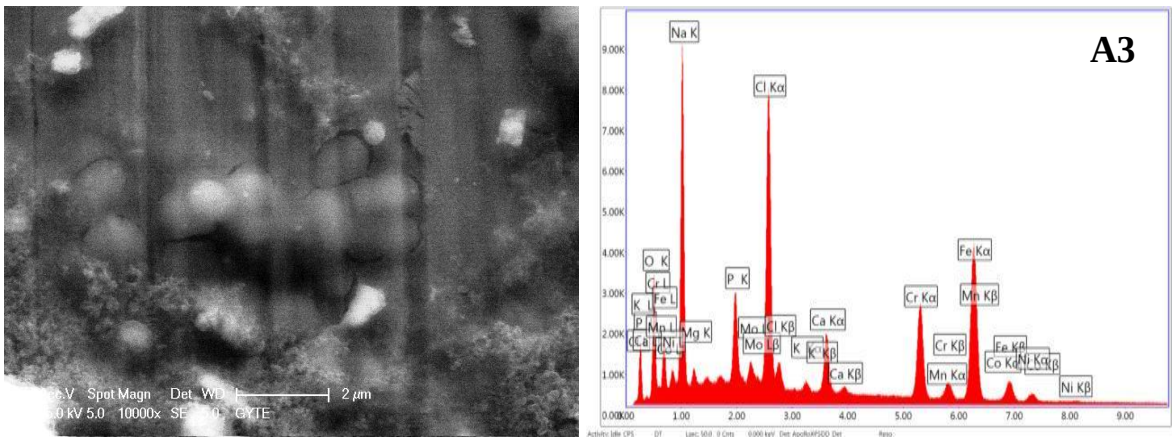

Figure 4. EDS analysis of the apatite formation occurring on the weld seam of the laser beam welded A1, A2 and A3 numbered samples on the surface of the A: base material which was soaked in the SBF for 28 days.

Upon determining that the surfaces of the all samples are fully and more densely covered with apatite minerals by means of SEM images at the end of the 28th day (Fig. 2 and Fig. 3), EDS inspection was carried out on any area of the non-welded samples and the weld seam of the laser welded samples which were immersed in the SBF for 28 days (Fig. 4).

As a result of the EDS inspections it was determined that Ca, P, O and Na elements were formed (Fig. 4). These are the main elements of hydroxyapatite, which is a bone-like apatite formation on the weld seam surface of the laser welded and non-welded samples. On the surface of the AISI 316L stainless steel base material, the Ca/P ratio as a result of 28 days of soaking in the SBF was calculated as being approximately 1.16; while Ca/P ratio of the weld seam of laser welded sample A1 was 1.04, and the Ca/P ratio of the weld seam sample A2 was 1.14 and Ca/P ratio of the weld seam sample A3 was 1.06 (weight %). After being immersed in SBF for 28 days, the apatite structure that particularly formed on weld seams was characterized with EDS and the value of the bioactive Ca and P ion ratios (Ca/P) was determined to be lower than 1.67, the stoichiometric Ca/P value, while the Ca/P ratios of the samples were determined to have proximal values.

Stoichiometric Ca/P ratio of hydroxyapatite is 1.67. When the deposited apatite layer Ca/P ratios are below 1.67 on the surfaces of the non-welded samples and on the weld seam of the laser beam welded AISI 316L stainless steel samples which are soaked in the SBF, this structure is referred to as carbonate-containing calcium-deficient hydroxyapatite with low crystallinity formation [9,39-41]. There are many kinds of HA and they are classified on the basis of Ca/P ratio [39]. Several chemical formulas have been proposed for calcium-deficient HA [3,39]. An example to the proposed formulas is $Ca_{10-x}(PO_4)_{6-2x}(HPO_4)_{2x}(OH)_2$, $0 < x < 2$ [3,39,42].

It is very important for base material and weld seam surface of laser welded sample to form adequate Ca and P deposition for positive development of the interaction between the implant surface and living bone tissue, and for bone tissue to be bonded to the implant surface. Also, coating of stainless steels with biocompatible minerals such as HA is an easy way of preventing corrosion of implants and enabling the long-time use of the metallic implants [43-45]. Austenitic stainless steel

AISI 316L stainless steel is one of the most popular and economical choices in despite of the potential risks related to release of toxic metallic ions in physiological environment [11] even though they are small in size and release of metallic ions can cause problems for people who are allergic to nickel or metal ions [11,40,46]. It is important for the implants are covered with hydroxyapatite in order to minimize the problems of people who are sensitive to metals [47].

3.3. Weight loss and corrosion resistance

Weight loss results of the laser beam welded and non-welded samples which were immersed in the SBF respectively for 1, 3, 7, 14, 21 and 28 days is presented in Fig. 5. It can be seen that the sample belonging to AISI 316L stainless steel base material had lower weight loss than samples joined at different laser welding travel speeds. This, in reality, is an expected outcome (Fig. 5).

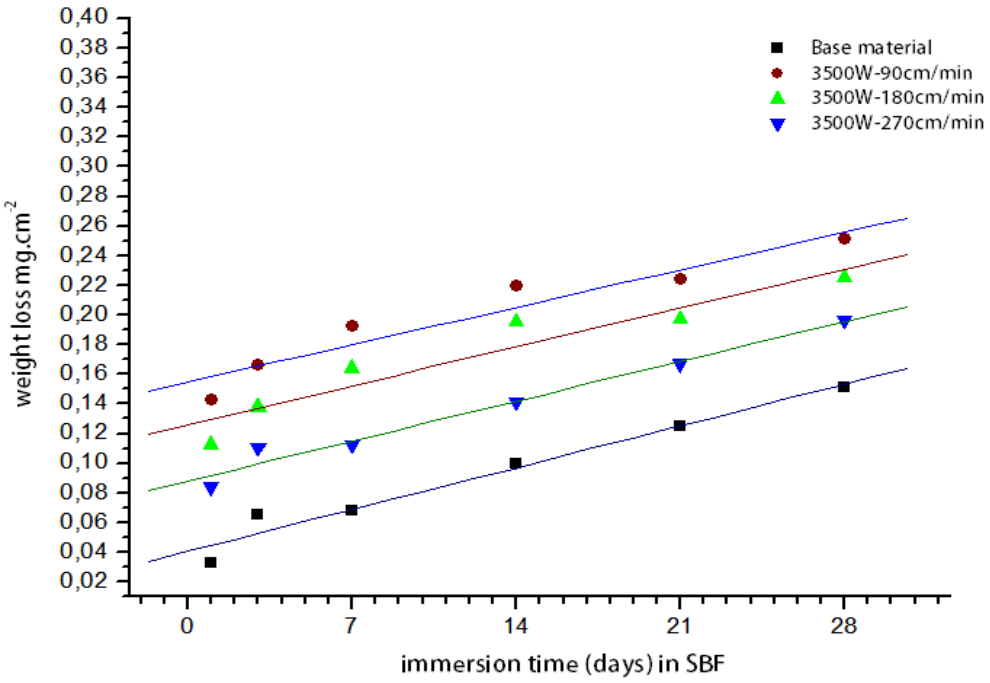

Figure 5. Weight loss rates of the base material and laser beam welded A1, A2 and A3 samples immersed in the SBF for 1-28 days.

It can be clearly seen from the results that weight loss occurs in proportion to the increase of the soaking period of the base material and laser welded samples in the SBF (Fig. 5). Although the AISI 316L stainless steel samples were joined through the laser beam welding method with low heat input, it is clear that the samples were, at least to small extent, affected from the welding thermal cycle and a sensitivity occurred in weld metal or HAZ in comparison to base material and that this sensitivity caused weight losses in the welded joints. However, it should be mentioned that the weight losses in question are in very small amounts. It can be seen that the heat input is the general factor that causes weight losses during the soaking period of the laser welded AISI 316L austenitic stainless steel

samples in the SBF. It was detected that the sample A3 which was joined with the lowest heat input (with 0.077 kJ/mm) had the minimum amount of weight loss and the sample A1 which was joined with the highest heat input (with 0.233 kJ/mm) had the maximum amount of weight loss. Protective thin oxide layer forming on the surface of the laser welded or non-welded samples enabled the samples to be stable against the weight loss in the SBF. Stainless steel formed a passive film layer (Fe, Ni)O(Fe, $Cr)_2O_3$ on the surface with the passivation process due to its chromium content. Molybdenum, however, increases the stability of the passive oxide layer and, therefore, the ability of the stainless steel to resist the corrosion environments, particularly in environments containing chloride ions [48,49].

Stainless steels have in common a good corrosion resistance in physiological environment, basically due to the formation of a thin passive oxide layer [27]. This oxide layer reduces the corrosion rate by blocking the migration of metal ions, enables the slowing down of corrosion rates and promotes the biocompatibility of metallic implants [25,50,51]. It has been understood from the weight loss results that both laser welded and non-welded samples of AISI 316L stainless steel samples displayed the required resistance with the chemical compositions, internal structures and surface properties they had while they were immersed in the SBF.

Body fluids may cause corrosion attacks on metallic implants due to their dense saline content [52]. SBF causes weight loss in the metallic materials as it can be seen from Fig. 5. Corrosion rates of the laser beam welded and non-welded samples which in the SBF, which are calculated based on their weight losses are presented in Fig. 6.

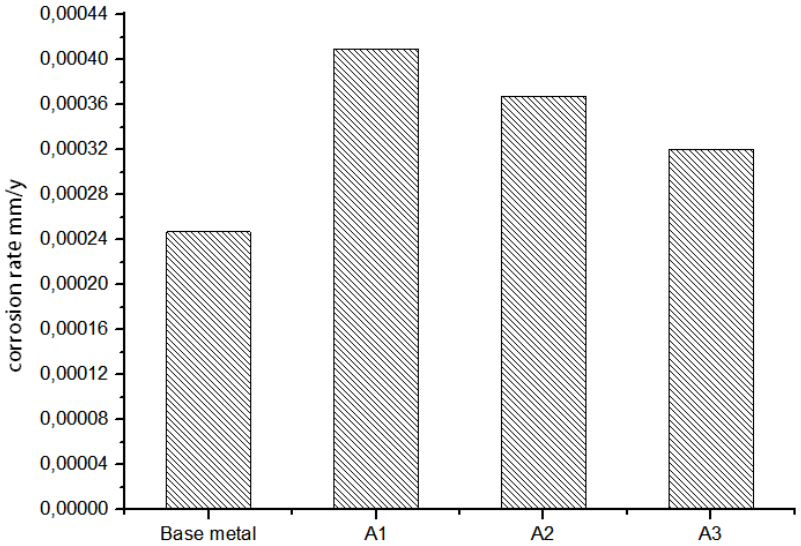

Figure 6. Corrosion rates of the base material and laser beam welded A1, A2 and A3 samples immersed in the SBF for 28 days.

It can be clearly seen from Fig. 6 that the corrosion rates of laser welded and base materials are at very low levels. It is thought that HA layer deposited on the surfaces of the samples causes the decrease in the corrosion rates, depending on the increase of the number of days during which laser welded and non-welded samples were kept soaking in the SBF.

Biocompatible HA coating can lead to delay in corrosion and wear [53,54]. HA coating provides shielding on stainless steel to prevent corrosion by acting as a barrier against the release of metal ions into corrosive and biological environment [55,56].

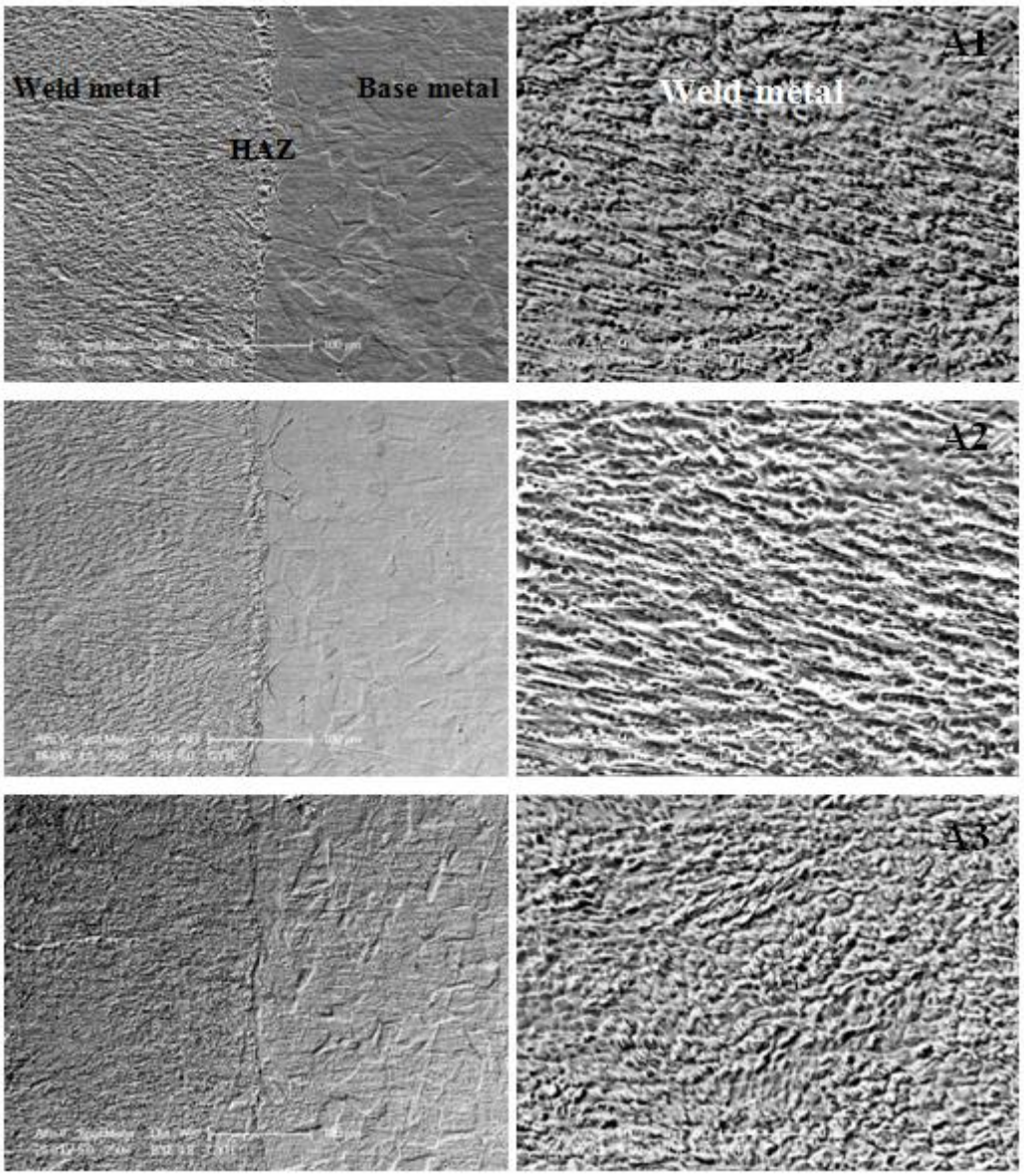

Figure 7. SEM images of the HAZ and weld metal areas of the laser beam welded A1, A2 and A3 samples immersed in the SBF for 28 days.

With the increase of soaking time in the SBF, the increase of the apatite layers deposited on the surface of the samples prevented the release of metallic ions and weight losses from the samples in the SBF environment, as well as decreasing the corrosion rates. Also, in the SEM images which show the apatite formation clearly on the samples (Fig. 2 and Fig. 3) it has been seen that the apatite layer did not fully cover the surfaces of the samples especially in the first days and weeks and this situation caused changes in corrosion rates of the samples in certain soaking periods. Since surfaces of the samples which were not fully covered with apatite were subjected to chloride ion attacks and became

sensitive, and the chromium oxide layer formed on the subject was locally disrupted, weight losses and accordingly, a small increase in the corrosion rates occurred [49]. In physiological systems, chloride is the most aggressive species by far [57]. At the same time, the cause for AISI 316L austenitic stainless steel laser welded or non-welded samples showing different corrosion resistances in the SBF is considered to occur from the chromium, nickel and molybdenum ratio differences in the chromium oxide layer and the difference of repassivation forming times.

SEM inspections have been carried out in the nitric acid (HNO_3) solution which was prepared for the removal of corrosion products that might have formed on the surfaces of the laser beam welded and non-welded AISI 316L stainless steel samples which were kept in the SBF for 28 days. As it can be understood from the SEM images, there were no formations indicating corrosion mechanisms (such as pits, cracks) in the areas of HAZ and weld metal of the laser beam welded A1, A2 and A3 samples (Fig. 7). SEM images supported the weight loss ratio and corrosion rate results.

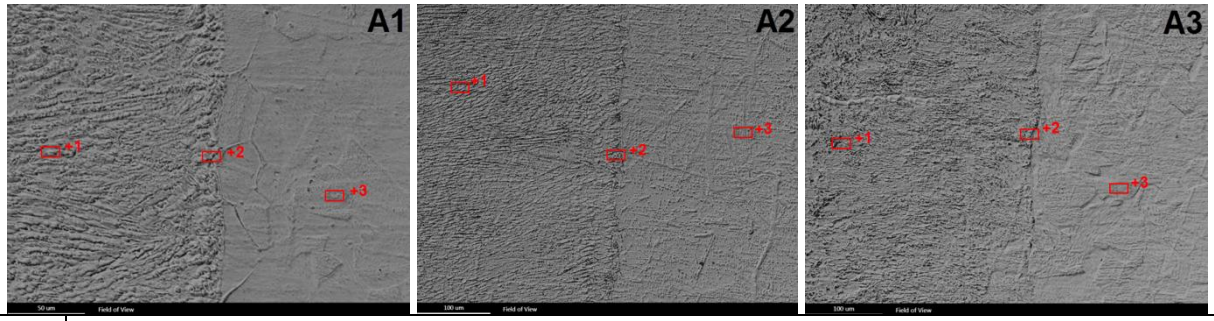

Sample code	Elements (weight %)											
	point number +1	Cr	Ni	Mo	point number +2	Cr	Ni	Mo	point number +3	Cr	Ni	Mo
A1	Base metal	16.18	9.29	1.31	HAZ	16.05	10.01	1.36	Weld metal	16.2	9.88	1.37
A2	Base metal	16.1	9.64	1.33	HAZ	15.62	9.23	1.1	Weld metal	16.01	9.78	1.36
A3	Base metal	16.05	9.02	1.39	HAZ	15.96	8.97	1.36	Weld metal	15.44	8.92	1.22

Figure 8. EDS analysis of the base metal, HAZ and weld metal area of the laser beam welded A1, A2 and A3 samples soaked in the SBF for 28 days.

If the oxide film layer covering the surface of a metallic implant materials is disrupted due to interaction with body fluids inside the body, the corrosion advances, and due to release of metallic ions, causes allergic reactions [53,55]. Release of chromium, nickel and molybdenum into the body from the stainless steel implant material may trigger local immune responses and inflammatory reactions [53,58]. Moreover, biocompatibility and osseointegration of the metallic implants suffering from corrosion are weakened and cause the implant to be mechanically damaged [51,53,59-61]. Thus, a biomaterial is required to have a low ion release rate in biomedical environments [60,62]. When the EDS analysis results of the laser welded samples which are immersed for 28 days in the SBF are inspected, it can be seen that no excessive element losses were experienced on the base material, HAZ

and weld metal area (Fig. 8). The elements of the samples which are immersed in the SBF stayed strongly stable and made the samples more resistant to corrosion.

A biomaterial should remain intact for a long period in a human body and should not fail until the death of the person in question [53]. A minimum service period of 15 to 20 years for older patients and more than 20 years for younger patients [53]. It has been concluded that the corrosion rates of AISI 316L base material and A1, A2 and A3 laser welded samples, which are joined with different weld speeds, to be used as implants in the human body are much lower values than tolerable corrosion rates. According to these results the view is that CO_2 laser beam welded AISI 316L austenitic stainless steel could be used in human body for short-term implants.

4. CONCLUSIONS

AISI 316L austenitic stainless steel have been used as prosthetics and implants in the biomedical industry due to their advanced mechanical strength, high corrosion resistance and biocompatibility [63-65]. Bioactivity properties and corrosion resistance of the CO_2 laser beam welded and non-welded AISI 316L austenitic stainless steel have been researched in this study and the conclusions are presented below:

- It was determined that weld seam surfaces of laser beam welded samples and non-welded samples which were soaked in the SBF started to be covered with apatite from day 1, and apatite formation was better on the surface of the base material than weld seam surface of laser beam welded samples. This situation could be explained by surface of the base material having better bioactive properties than weld seam surface of laser beam welded samples. Bioactivity properties, in particular, might have been affected by the welding thermal cycle and chromium oxide film characteristics.
- Based on the EDS analysis results taken from the apatite covered base material surface and the weld seam of laser beam welded samples, it was determined that the Ca/P ratio is lower than the stoichiometric ratio of bones, which is 1.67. Surface of the samples were covered with apatite minerals which are referred to as carbonate-containing calcium-deficient hydroxyapatite with low crystallinity formations. Apatitic calcium layer formation on the surface of non-welded and laser beam welded samples increased as periods of immersion were extended; the calculations displayed similar Ca/P ion concentrations on surfaces of all samples.
- The apatite increase amount, weight loss and corrosion rate were mainly affected by the heat input. Laser beam welded and non-welded AISI 316L austenitic stainless steel samples which were immersed in the SBF for 1 to 28 days were determined to have lower weight loss, and due to that, their corrosion rate was found to be very low. This situation indicates that laser beam welded samples would present enough corrosion resistance when used as implants in the human body. Especially after the soaking period of laser beam welded samples A1, A2 and A3 for 28 days in the SBF, SEM images taken from the main material, HAZ and weld seam, and EDS analysis supported this view as well.

- Laser beam welded AISI 316L austenitic stainless steel may be proposed for short term or long term in vitro cell culture clinical studies and in vivo applications.

ACKNOWLEDGEMENT
The authors acknowledge Karabuk University, Project and Science Research Commission for their support. Form laser Company is also acknowledged for the laser welding process.

References

1. E.P. Ivanova, K. Bazaka, and R.J. Crawford, *New Functional Biomaterials for Medicine and Healthcare*, 1st edition, Woodhead Publishing. Sawston (2014)
2. J.R. Davis, *Stainless Steels*, ASM international, Materials Park, Ohio (1994)
3. Ó. Martín, P. De Tiedra, C. García, F. Martín, and M. López, *Corrosion Science*, 54 (2012) 126
4. A. Balamurugan, S. Rajeswari, G. Balossier, A.H.S. Rebelo, and J.M.F. Ferreira, *Materials and Corrosion*, 59 (2008) 869
5. C.C. Shih, C.M. Shih, K.Y. Chou, S.J. Lin, and Y.Y. Su, *Journal of Biomedical Materials Research Part A*, 80 (2007) 873
6. D. Kuroda, S. Hiromoto, T. Hanawa, and Y. Katada, *Materials Transactions*, 43 (2002) 3104
7. Y.C. Tang, S. Katsuma, S. Fujimoto, and S. Hiromoto, *Acta Biomaterialia*, 2 (2006) 715
8. C.P.O. Ossa, S.O. Rogero, and A.P. Tschiptschin, *J Mater Sci. Mater Med*, 17 (2006) 1100
9. X. Fan, J. Chen, J.P. Zou, Q. Wan, Z.C. Zhou, and J.M. Ruan, *Transactions of Nonferrous Metals Society of China*, 19 (2009) 352
10. S. Sutha, K. Kavitha, G. Karunakaran, and V. Rajendran, *Materials Science and Engineering C*, 33 (2013) 4054
11. V.K. Balla, M. Das, S. Bose, G.D. Ram, and I. Manna, *Materials Science and Engineering C*, 33 (2013) 4598
12. A. Karakaş, A.B. Hazar Yoruç, D. Ceylan Erdoğan, and M. Doğan, *Acta Physica Polonica-Series A General Physics*, 121 (2012) 236
13. S. Durdu, and M. Usta, *Ceramics International*, 40 (2014) 3635
14. M. Markovic, B.O. Fowler, and M.S. Tung, *Journal of Research of The National Institute of Standards and Technology*, 109 (2004) 568
15. A. Oyane, X. Wang, Y. Sogo, A. Ito, and H. Tsurushima, *Acta Biomaterialia*, 8 (2012) 2046
16. E. Mohseni, E. Zalnezhad, and A.R. Bushroa, *International Journal of Adhesion and Adhesives*, 48 (2014) 257
17. V.P. Orlovskii, V.S. Komlev, and S.M. Barinov, *Inorganic Materials*, 38 (2002) 984
18. H.R. Bakhsheshi-Rad, E. Hamzah, M. Daroonparvar, M. Kasiri-Asgarani, M. Medraj, *Ceramics International*, 40 (2014) 14018
19. D.A. Wahl, and J.T. Czernuszka, *Eur Cell Mater*, 11 (2006) 56
20. A. Zadpoor, *Materials Science and Engineering C*, 35 (2014) 143
21. M. Fini, N. Nicoli, P. Toricelli, G. Giaveresi, *Biomaterials*, 24 (2003) 4939
22. N. Hallab, K. Merritt, and Jacobs JJ, *The Journal of Bon & Joint Surgery*, 83 (2001) 428
23. A. Choubey, B. Basu, and R. Balasubramaniam, *Trends Biomater, Artif. Organs*,18 (2005) 72
24. I. Gurappa, , 49 (2002) 79
25. D.A. Lopez, A. *Materials Characterization* Duran, and S.M. Cere, *J Mater Sci. Mater Med, Springer*, 19 (2007) 2137
26. C. Köse, and R. Kaçar, *Materials & Design*, 64 (2014) 226
27. C. Köse, and R. Kaçar, *Materials Testing*, 56 (2014) 785

28. M. Taskin, U. Caligulu, and M. Turkmen, *Materials Testing*, 53 (2011) 741
29. W.W. Duley, *Laser Processing and Analysis of Materials*, Plenum Press., New York (1983)
30. A. Ruggiero, L. Tricarico, A.G. Olabi, and K.Y. Benyounis, *Optics & Laser Technology*, 43 (2011) 90
31. C. Köse, and R. Kaçar, *Journal of the Faculty of Engineering and Architecture of Gazi University*, 30 (2015) 235
32. ASTM G1-03-E, *Standard Practice for Preparing, Cleaning, and Evaluation Corrosion Test Specimens*, American Society for Testing and Materials (1999)
33. T. Kokubo, and H. Takadama, *Biomaterials*, 27 (2006) 2915
34. C. Köse, and R. Kaçar, *The Second International Iron and Steel Symposium (IISS'15)*, Karabuk, Turkey
35. M.R. Marques, R. Loebenberg, and M. Almukainzi, *Dissolution Technol.*, 18 (2001) 28
36. J.H. Park, D.Y. Lee, K.T. Oh, Y.K. Lee, K.M. Kim, and K.N. Kim, *Materials Letters*, 60 (2006) 2577
37. T. Kokubo, *Journal of Non-Crystalline Solids*, 120 (1990) 151
38. M. Theiszova, S. Jantova, J. Dragunova, P. Grznarova, and M. Palou, *Biomedical Papers-Palacky University in Olomouc*, 149 (2005) 393
39. K. Byrappa, and T. Ohachi, *Crystal Growth Technology*, *Cheapter 16*, *Growth of Hydroxyapatite Crystals*-Atsuo Ito and Kazuo Onuma, William Andrew Publishing, NewYork (2006)
40. M. Sasaki, M. Inoue, Y. Katada, Y. Nishida, A. Taniguchi, S. Hiromoto, and T. Taguchi, *Science and Technology of Advanced Materials*, 13 (2012) 8
41. S. Yu, K.P. Hariram, R. Kumar, P. Cheang, K.K. Aik, *Biomaterials*, 26 (2005) 2352
42. A.C. Tas, and S.B. Bhaduri, *Journal of Materials Research*,19 (2004) 2749
43. X. Lu, and Y. Leng Y, *Biomaterials*, 26 (2005) 1108
44. C.T. Kwok, P.K. Wong, F.T. Cheng, and H.C. Man, *Applied Surface Science*, 255 (2009) 6744
45. A. Tahmasbi Rad, M. Solati-Hashjin, N.A.A. Osman, and S. Faghihi, *Ceramics International*, 10 (2014) 12691
46. P. Wan, Y. Ren, B. Zhang, K. Yang, *Materials Science and Engineering C*, 32 (2012) 516
47. M. Dinçer, D. Teker, P. Sağ Can, and K. Öztürk, *Surface & Coatings Technology*, 226 (2013) 33
48. M. Conradi, P.M. Schön, A. Kocijan, M. Jenko, and G.J. Vancso, *Materials Chemistry and Physics*,130 (2011) 713
49. E.F. Pieretti, and I. Costa, *Electrochimica Acta*, 114 (2013) 843
50. J. Ballarre, I. Manjubala, W.H. Schreiner, J.C. Orellano, P. Fratzl, and S. Ceré, *Acta Biomaterialia*, 6 (2010) 1609
51. T. Hryniewicz, K. Rokosz, and R. Rokicki, *Corrosion Science*, 50 (2008) 2681
52. F. Rubitschek, T. Niendorf, I. Karaman, H.J. Maier, *Journal of the Mechanical Behavior of Biomedical Materials*, 5 (2012) 192
53. G. Manivasagam, D. Dhinasekaran, and A. Rajamanickam, *Recent Patents on Corrosion Science*, *Bentham Open*, 2 (2010) 54
54. K.K. Chew, S.H.S. Zein, A.L. Ahmad, *Natural Science*, 4 (2012) 184
55. D.C. Hansen, *The Electrochemical Society Interface* , 17 (2008) 31
56. M. Mhaede, A. Ahmed, M. Wollmann, L. Wagner, *Materials Science and Engineering C*, 50 (2015) 30
57. G.T. Burstein, and C. Liu, *Corrosion Science*, 49 (2007) 4306
58. M. Cieślik, K. Engvall, J. Pan, and A. Kotarba, *Corrosion Science*, 53 (2011) 301
59. K. Yaya, Y. Khelfaoui, B. Malki, M. Kerkar M, *Corrosion Science*, 53 (2011) 3314
60. L. Wang, J.F. Su, and X. Nie, *Surface and Coatings Technology*, 205 (2010) 1605
61. I. E. Castañeda, J.G. Gonzalez-Rodriguez, G. Dominguez-Patiño, R. Sandoval-Jabalera, M.A.Neri-Flores, JG. Chacon-Nava, A. Martinez-Villafañe, *Int. J. Electrochem. Sci.*, 6 (2011) 405
62. Y. Xu, Y. Xiao, D. Yı, H. Liu, L. Wu, J. Wen, *Trans. Nonferrous Met. Soc. China*, 25 (2015) 2563

63. C. Köse, R. Kaçar, A.P. Zorba, M. Bağırova, and A.M. Allahverdiyev, *Materials Science and Engineering C*, 60 (2016) 218
64. D. Özyürek, *Materials and Design*, 29 (2008) 597
65. R. Yılmaz, and M. Tümer, *Int J Adv Manuf Technol*., 67 (2013) 1433